Molecular Biology of the Cell
Vol. 20, 2810–2819, June 15, 2009

Down-Regulation of a Manganese Transporter in the Face of Metal Toxicity

Laran T. Jensen,* Mark C. Carroll,* Matthew D. Hall,*† Christopher J. Harvey,* Sara E. Beese,‡ and Valeria C. Culotta*

*Department of Environmental Health Sciences and ‡Department of Biochemistry and Molecular Biology, Johns Hopkins University Bloomberg School of Public Health, Baltimore, MD 21205

Submitted October 30, 2008; Revised March 24, 2009; Accepted April 8, 2009
Monitoring Editor: Patrick J. Brennwald

The yeast Smf1p Nramp manganese transporter is posttranslationally regulated by environmental manganese. Smf1p is stabilized at the cell surface with manganese starvation, but is largely degraded in the vacuole with physiological manganese through a mechanism involving the Rsp5p adaptor complex Bsd2p/Tre1p/Tre2p. We now describe an additional level of Smf1p regulation that occurs with toxicity from manganese, but not other essential metals. This regulation is largely Smf1p-specific. As with physiological manganese, toxic manganese triggers vacuolar degradation of Smf1p by trafficking through the multivesicular body. However, regulation by toxic manganese does not involve Bsd2p/Tre1p/Tre2p. Toxic manganese triggers both endocytosis of cell surface Smf1p and vacuolar targeting of intracellular Smf1p through the exocytic pathway. Notably, the kinetics of vacuolar targeting for Smf1p are relatively slow with toxic manganese and require prolonged exposures to the metal. Down-regulation of Smf1p by toxic manganese does not require transport activity of Smf1p, whereas such transport activity is needed for Smf1p regulation by manganese starvation. Furthermore, the responses to manganese starvation and manganese toxicity involve separate cellular compartments. We provide evidence that manganese starvation is sensed within the lumen of the secretory pathway, whereas manganese toxicity is sensed within an extra-Golgi/cytosolic compartment of the cell.

INTRODUCTION

Metals that are both essential and potentially toxic pose a challenge to cells in that sufficient quantities must be acquired in times of metal starvation, whereas hyperaccumulation must be minimized in times of metal surplus. To help meet this challenge, the levels and/or cellular localization of metal transporters are often regulated in response to changes in metal exposures. In studies that have been conducted in yeast, transporters for zinc, copper, and iron are all induced at the level of transcription by metal responsive transcription factors (Jungmann *et al.*, 1993; Yamaguchi-Iwai *et al.*, 1996; Iwai *et al.*, 1997; Zhao and Eide, 1997; Dancis, 1998). Yet thus far, no transcriptional regulation has been described for transporters of manganese. Instead, the major manganese transporters of yeast, Smf1p and Smf2p, are regulated at the posttranslational level.

Smf1p and Smf2p are members of a well-conserved family of Nramp metal transporters that from bacteria to humans are involved in the uptake and distribution of iron, manganese, and other divalent metals (Cellier *et al.*, 1995; Gunshin *et al.*, 1997; Thomine *et al.*, 2000). Although Smf1p and Smf2p are both manganese transporters in yeast, they are not redundant in function. Smf2p is largely responsible for the activation of manganese enzymes in the cell (Luk *et al.*, 2005), whereas Smf1p is more critical for oxidative stress protection by supplying the cell with critical manganese antioxidants (Reddi *et al.*, 2009). With normal physiological levels of manganese, a large fraction of Smf1p and Smf2p are subject to rapid turnover by degradation in the vacuole (Liu and Culotta, 1999b; Portnoy *et al.*, 2000). This continual degradation of Smf1p and Smf2p maintains these transporters at a low steady-state level that is sufficient for essential manganese acquisition but prohibits excess transport of other toxic metals (Liu *et al.*, 1997).

The vacuolar degradation of Smf1p and Smf2p during physiological manganese has been well characterized. In the secretory pathway, the bulk of newly synthesized Smf1p and Smf2p are recognized by Tre1p/Tre2p and Bsd2p, which triggers ubiquitination of the transporters via Rsp5p. Ubiquitinated Smf1p and Smf2p then enter the multivesicular body (MVB) pathway for delivery to the vacuolar lumen for degradation (Liu *et al.*, 1997; Liu and Culotta, 1999b; Portnoy *et al.*, 2000; Eguez *et al.*, 2004; Hettema *et al.*, 2004; Stimpson *et al.*, 2006; Sullivan *et al.*, 2007). Yet during manganese starvation, this down-regulation of Smf1p and Smf2p is abrogated. The transporter polypeptides fail to be recognized by Tre1p/Tre2p and Bsd2p and rather than vacuolar targeting, the bulk of Smf1p and Smf2p relocate to the cell surface and intracellular vesicles to optimize manganese uptake and distribution (Liu and Culotta, 1999b; Luk and Culotta, 2001; Sullivan *et al.*, 2007). The mechanism for the switch in Smf1p and Smf2p localization is currently unknown, but has been proposed to involve manganese binding directly to the transporters (Liu and Culotta, 1999a; Sullivan *et al.*, 2007).

This article was published online ahead of print in *MBC in Press* (http://www.molbiolcell.org/cgi/doi/10.1091/mbc.E08–10–1084) on April 15, 2009.

† Present address: Laboratory of Cell Biology, National Cancer Institute, National Institutes of Health, Bethesda, MD 20892.

Address correspondence to: Laran T. Jensen (ljensen@jhsph.edu).

Abbreviations used: MVB, multivesicular body.

In addition to up-regulation by metal starvation, many metal transporters are down-regulated in response to metal toxicity. For example, yeast transporters for zinc, copper, and iron are turned over when cells are challenged with high doses of these metal ions (Gitan and Eide, 2000a; Gitan *et al.*, 2003; Petris *et al.*, 2003; Felice *et al.*, 2005; Liu *et al.*, 2007; Strochlic *et al.*, 2008). In all three cases, high concentrations of metal stimulate ubiquitination and endocytosis of the cell surface transporter and targeting to the vacuole for degradation. The Smf1p and Smf2p transporters can contribute to metal ion toxicity (Liu *et al.*, 1997), and recently cadmium has been shown to promote endocytosis of Smf1p through Rsp5p-dependent ubiquitination of specific lysine residues in the N-terminus (Nikko *et al.*, 2008). The regulation of Smf1p by cadmium was mediated by several arrestin-like proteins that appear to function as Rsp5p adaptors. However the regulation of Smf1p by cadmium appeared distinct from previously reported regulation of this transporter, because endocytosis was not observed when cells were stressed with manganese (Nikko *et al.*, 2008), and additional down-regulation of Smf1p and Smf2p in response to manganese toxicity has not been previously reported.

In this study, we have examined the fate of the Smf1p manganese transport protein in response to manganese starvation, physiological manganese, and manganese toxicity. We report here that in addition to the "basal" down-regulation of Smf1p during physiological manganese, an additional tier of Smf1p down-regulation occurs when cells are subject to very high doses of the metal. Loss of Smf1p at toxic manganese is distinct from Bsd2p-dependent regulation of the protein, but nevertheless does involve vacuolar degradation through the MVB pathway. We observe that sensing of manganese for regulating Smf1p at very low and very high metal levels requires distinct intracellular pools of the metal.

MATERIALS AND METHODS

Plasmids, Strains, and Growth Conditions

The majority of yeast of strains used in this study were derived from BY4741 (*Mata, leu2Δ0, met15Δ0, ura3Δ0, his3Δ1*). Single gene deletions strains in the BY4741 background including *bsd2Δ::kanMX4, tul1Δ::kanMX4, pmr1Δ::kanMX4,* and *mam3Δ::kanMX4* were obtained from Research Genetics (Huntsville, AL). The *BSD2* gene was deleted in the indicated *kanMX4* disruption strains using the *bsd2Δ::HIS3* deletion plasmid (Liu *et al.*, 1997) resulting in LJ385 (*bsd2Δ::HIS3 vps21Δ::kanMX4*), LJ386 (*bsd2Δ::HIS3 snf7Δ::kanMX4*), LJ387 (*bsd2Δ::HIS3 vps36Δ::kanMX4*), LJ388 (*bsd2Δ::HIS3 pep4Δ::kanMX4*), LJ389 (*bsd2Δ::HIS3 vps4Δ::kanMX4*), LJ390 (*bsd2Δ::HIS3 vps23Δ::kanMX4*), LJ391 (*bsd2Δ::HIS3 vps27Δ::kanMX4*), LJ392 (*bsd2Δ::HIS3 end3Δ::kanMX4*), LJ393 (*bsd2Δ::HIS3 vps45Δ::kanMX4*), LJ395 (*bsd2Δ::HIS3 pep12Δ::kanMX4*), LJ404 (*bsd2Δ::HIS3 apm3Δ::kanMX4*), LJ405 (*bsd2Δ::HIS3 atg1Δ::kanMX4*), LJ424 (*pRSP5Δ::HIS3*), LJ426 (*bsd2Δ::kanMX4, pep4Δ, pRSP5Δ::HIS3*). Additional strains used include BY4742 (*Matα, leu2Δ0, lys2Δ0, ura3Δ0, his3Δ1*), the *tre1/2Δ* strain (*Matα, leu2Δ0, lys2Δ0, ura3Δ0, his3Δ1, tre1Δ, tre2Δ::kanMX4*; Stimpson *et al.*, 2006), LJ420 (*tre1/2Δ bsd2Δ::HIS3*), and LJ423 (BY4742 *bsd2Δ::HIS3*), LJ431 (*his3, trp1, lys3, ura3, leu2, bar1, bsd2Δ::LEU2*), LJ432 (*his3, trp1, lys3, ura3, leu2, bar1, rsp5-1, bsd2Δ::LEU2*) isogenic to LHY291 and LHY23, respectively (Dunn and Hicke, 2001) and the *sod1Δ bsd2Δ smf1-1* strain XBSBS1 (Liu *et al.*, 1997). Yeast transformations were performed using the lithium acetate procedure (Gietz and Schiestl, 1991). Cells were propagated at 30°C unless otherwise specified either in enriched yeast extract, peptone-based medium supplemented with 2% glucose (YPD), synthetic complete (SC) medium (Sherman *et al.*, 1978) or in a metal-depleted minimal defined medium prepared through use of an ion exchange resin (Dancis *et al.*, 1990).

Plasmids pSF4 (*SMF1*), pSF6 (*SMF2*), and pMP043 (*SMF3*) expressing hemaglutinin (HA)-tagged versions of Smf1p, Smf2p, and Smf3p have been described previously (Liu and Culotta, 1999a,b; Portnoy *et al.*, 2000). In all cases, the HA tag is placed at the C-terminus. Point mutations in *SMF1* were generated using pSF4 (Smf1-HA) as a template resulting in plasmids D92GpSF4, N95TpSF4, and E344ApSF4. The *SMF1* promoter *lacZ* fusion plasmid was constructed using a derivative of pSF4 with a BamHI site immediately after the start codon. The *SMF1* promoter was excised as an XhoI to BamHI fragment and ligated into the ß-galactosidase reporter plasmid pLGΔ178 (Guarente and Mason, 1983) cut with the same enzymes generating plasmid pLJ389 (containing *SMF1* sequences −296 to + 1). The GFP-Smf1 plasmid was a generous gift from Hugh Pelham (MRC Laboratory of Molecular Biology) and expresses a N-terminal GFP-Smf1 fusion in YCplac33 (*CEN URA3*) using the *TPI1* promoter (Sullivan *et al.*, 2007). To generate N-terminal GFP fusions of *SMF2* and *SMF3* driven by the *TPI1* promoter, *SMF1* was excised from the GFP-SMF1 plasmid with BamHI and XbaI and replaced with *SMF2* or *SMF3* resulting in plasmids pLJ433 (GFP-SMF2) and pLJ434 (GFP-SMF3). A N-terminal truncation of *SMF1* was also generated in GFP-Smf1 by introducing a BamHI site at codon 63 followed by digestion with BamHI and religating resulting in plasmid pLJ365. A K33, 34R derivative of GFP-Smf1 was generated by site-directed mutagenesis resulting in plasmid pLJ460. To express C-terminal GFP fusions of *FUR4* and *TAT2* driven by the *PGK1* promoter, *FUR4* (−19 to + 1899) and *TAT2* (−17 to + 1776), sequences were PCR amplified using Pfu polymerase introducing 5′ SpeI or XbaI sites respectively, and replacing the stop codons with NotI sites. The PCR products were digested with the appropriate enzymes and ligated into plasmid pLJ457, a derivative of pAA1 (Hobbs *et al.*, 2001) but containing a GFP fusion with *PHO84* driven by the *PGK1* promoter with a *URA3* selectable marker, digested with XbaI/NotI, replacing the *PHO84* sequences with those for either *FUR4* or *TAT2,* resulting in plasmids pLJ458 and pLJ459, respectively. The *RSP5* promoter disruption plasmid pLJ461 was generated by PCR, amplifying upstream (−916 to −468) and downstream sequences (−9 to +508) of *RSP5,* introducing XbaI and EcoRI (upstream) or SacI and XbaI (downstream) restriction sites. After digestion the PCR products were ligated into pRS403 (*HIS3*; Sikorski, 1989) cut with SacI and EcoRI. All mutations were generated using the QuickChange mutagenesis kit (Stratagene, La Jolla, CA), and the sequence integrity of plasmids was ensured by double-stranded DNA sequencing (DNA Analysis Facility, Johns Hopkins University).

Immunoblots

Cultures were grown aerobically in either YPD or in minimal defined medium depleted of manganese that was supplemented as needed with $MnCl_2$. Cultures were innoculated at an $OD_{600\ nm}$ of 0.2 and grown for 16 h or grown to an $OD_{600\ nm}$ of ~1 before addition of $MnCl_2$. Yeast extracts were generated with the glass bead lysis protocol (Lapinskas *et al.*, 1996) using 10 mM NaH_2PO_4, 1% Triton X-100, 50 mM NaCl, 5 mM EDTA, 5 mM EGTA, pH 7.8, containing protease inhibitors. Proteins were separated by SDS-PAGE using 12% gels, and immunoblots were probed with either anti-HA (Roche, Indianapolis, IN), anti-GFP (Molecular Probes, Eugene, OR), or anti-Pgk1 (Molecular Probes) antibodies at a 1:5000 dilution. Visualization of immunoblots utilized either HRP-conjugated secondary antibodies with ECL detection (Amersham Pharmacia Biotech, Piscataway, NJ) or the Odyssey infrared imagining system (Li-Cor Biosciences, Lincoln, NE) employing an Alexa Fluor 680 secondary antibody (Invitrogen, Carlsbad, CA). Quantitation of immunoblots utilized Odyssey quantitation software (version 1.2).

ß-Galactosidase Assays

Yeast transformants expressing either the p*SMF1* or p*ACT1 LacZ* reporter constructs were grown in YPD medium and ß-galactosidase activities were assayed using *o*-nitrophenyl ß-D-galactopyranoside as a substrate as previously described (Portnoy *et al.*, 2002). Results from two independent transformants assayed at least in duplicate were reported in Miller units (Giacomini *et al.*, 1992).

Fluorescence Imaging

Cells expressing the green fluorescent protein (GFP)-SMF fusion were imaged essentially as described (Sundin *et al.*, 2004). A pad of 1% low melting agarose (United States Biological , Swampscott, MA) in YPD was generated by placing 40 μl of the melted agarose on a microscope slide and by compressing with a second slide. After agarose solidification and removal of the compressing slide, ~5×10^4 cells were placed on the pad and covered with a coverslip. Fluorescence was viewed directly with either a Zeiss Axioplan upright microscope (Thornwood, NY; The Johns Hopkins Integrated Imaging Center) or a Nikon Eclipse TE300 equipped with a digital monochrome cameras (Melville, NY) at 100× magnification.

RESULTS

The Down-Regulation of Smf1p by Toxic Manganese

Smf1p is known to respond to the switch from manganese starvation to physiological manganese by degrading much of the newly synthesized protein in the vacuole (Liu *et al.*, 1997; Liu and Culotta, 1999b; Eguez *et al.*, 2004; Hettema *et al.*, 2004; Stimpson *et al.*, 2006; Sullivan *et al.*, 2007). In addition to this well-defined pathway of Smf1p degradation under physiological manganese conditions, we now show that Smf1p is subject to down-regulation by toxic manganese. These two stages of Smf1p regulation are shown in

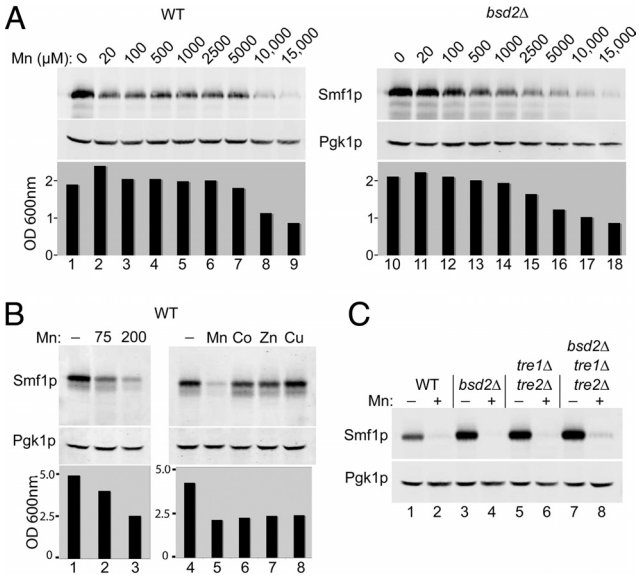

Figure 1. Smf1p is down-regulated by toxic manganese stress independently of Bsd2p. (A) WT or *bsd2*Δ yeast expressing GFP-Smf1 were grown for 16 h in a minimal defined medium depleted of manganese (Liu and Culotta, 1999b) and supplemented where indicated with the indicated concentration of $MnCl_2$ (μM). GFP-Smf1 levels were assayed using immunoblots, and Pgk1p was monitored as a loading control (top panels) with total growth assayed using the optical density of cultures (OD 600 nm; bottom panels). (B) Smf1-HA levels were monitored in WT cells grown for 16 h in enriched medium (YPD) supplemented with the indicated metal. Cultures contained no added metal (−), 75 or 200 μM $MnCl_2$ (left panel), and 500 μM $CoSO_4$, 200 μM $MnCl_2$, 1 mM $ZnCl_2$, or 7 mM $CuSO_4$ (right panel). (C) Immunoblot analysis of GFP-Smf1 from *bsd2*Δ, *tre1*Δ *tre2*Δ, and *bsd2*Δ *tre1*Δ *tre2*Δ strains. Cultures were grown for 16 h in YPD with no added metal (−) or 200 μM $MnCl_2$ (+). Strains utilized include WT, BY4741; *bsd2*Δ, 5738, *bsd2*Δ, LJ423; *tre1*Δ *tre2*Δ, *tre1/2*; and *bsd2*Δ *tre1*Δ *tre2*Δ, LJ420.

Figure 1A. The abundance of Smf1p tagged at the N-terminus with GFP ("GFP-Smf1") is high in manganese-deficient medium compared with growth in the same minimal medium supplemented with 20 μM manganese (Figure 1A, left, cf. lanes 1 and 2). Adding increasing levels of manganese up to 5 mM does not change GFP-Smf1 levels, nor does the metal cause substantial toxicity over these several orders of magnitude concentrations (Figure 1A, cf. lanes 2–7 and total growth bars below). We refer to this large range of nontoxic metal concentrations as "physiological" manganese. Yet when manganese in the growth medium becomes toxic to the cell, GFP-Smf1 levels are further decreased (Figure 1A, lanes 8 and 9). The down-regulation of Smf1 by toxic manganese is not medium specific and also occurs in enriched medium, the only difference being the effective dose. The toxic dose of manganese is much lower in enriched medium, as cells are far more efficient at accumulating the metal from enriched medium, perhaps because of formation of extracellular manganese-phosphate complexes (Yang *et al.*, 2005). As seen in Figure 1B, lanes 1–3, the level of a Smf1p tagged at the C-terminus with HA "Smf1-HA" from cells grown in enriched medium drops significantly as manganese levels begin to inhibit growth (see total growth bars below), and the same regulation at toxic manganese was observed with GFP-Smf1 (Figure 1C, lane 2).

The effect of high manganese on Smf1p does not reflect nonspecific growth inhibitory effects of metals. In Figure 1B, lanes 6–8 cells were treated with concentrations of cobalt, zinc, and copper that similarly inhibit total cell growth by ≈50% over a period of 16 h. Only manganese caused loss of Smf1-HA; if anything, copper treatment increased levels of Smf1-HA (lane 8), through an unknown pathway. We also tested whether the regulation of Smf1p by toxic manganese involves the Bsd2p and Tre1/Tre2 proteins implicated in Smf1-regulation by physiological manganese (Liu *et al.*, 1997; Stimpson *et al.*, 2006). As seen in Figures 1, A (right) and C, regulation of GFP-Smf1 by toxic manganese is preserved in a *bsd2*Δ strain. The same is true of GFP-Smf1 expressed in a triple *bsd2*Δ *tre1*Δ *tre2*Δ strain (Figure 1C). Hence, regulation of Smf1p at very high manganese is distinct from regulation by low manganese in that it does not involve Bsd2p and the Tre1 and Tre2 proteins.

Toxic manganese regulation of Smf1p occurs independent of the gene promoter. *SMF1* exhibits manganese regulation when driven by either its native promoter (sequences from −296; Figure 1B) or the nonnative *TPI1* promoter (Figure 1C). Moreover, when *SMF1* promoter sequences were fused to *LacZ*, there was no down-regulation of promoter activity by high manganese (Figure 2A). *SMF1* is not transcriptionally regulated by toxic manganese, and we therefore examined posttranscriptional effects. The Bsd2p-dependent regulation of Smf1p occurs through vacuolar degradation (Liu and Culotta, 1999b), and we tested whether the same was true for Bsd2-independent regulation. GFP-Smf1 protein levels were monitored in a *bsd2*Δ strain also containing a *pep4*Δ mutation blocking vacuolar proteases. As seen in Figure 2B, down-regulation of GFP-Smf1 by toxic manganese was inhibited in the *bsd2*Δ *pep4*Δ strain. By comparison, mutants that affect endoplasmic reticulum-associated degradation (ERAD) via the proteosome had no effect on toxic manganese regulation of GFP-Smf1 (Supplemental Figure S1). Visualizing GFP-Smf1 in the *bsd2*Δ *pep4*Δ strain clearly shows GFP-Smf1 localization changing from a combination of plasma membrane and vesicular localization under physiological manganese to accumulation in the vacuole in the presence of toxic manganese (Figure 2C). Hence regulation by both physiological (Bsd2p-dependent) and toxic manganese (Bsd2p-independent) involves targeting of the protein to the vacuole for degradation.

Three pathways for vacuolar targeting in yeast involve trafficking through multivesicular bodies (MVB), autophagy, and the pathway used by alkaline phosphatase (ALP; reviewed in Huang *et al.*, 2007 and references therein). To test which if any of these were involved in toxic manganese regulation of Smf1p, we created double *bsd2*Δ *vps4*Δ (blocking the MVB pathway), *bsd2*Δ *atg1*Δ (blocking autophagy), and *bsd2*Δ *apm1*Δ (blocking ALP) mutants. As seen in Figure 2D, toxic manganese regulation was prevented by a *vps4*Δ mutation in the MVB pathway, but not by mutants affecting autophagy or trafficking of ALP. An inspection of GFP-Smf1 localization in a *bsd2*Δ *vps4*Δ strain yielded a large punctate staining pattern reminiscent of class E compartments (Supplemental Figure S2) that are hallmarks of a block in trafficking through the MVB pathway (Raymond *et al.*, 1992). Therefore as is the case with Bsd2-dependent regulation of Smf1p (Hettema *et al.*, 2004; Sullivan *et al.*, 2007), Bsd2-independent regulation at toxic manganese involves trafficking to the vacuole through the MVB.

To verify that the enhanced stability of Smf1p in the presence of toxic manganese was not specific for *vps4*Δ cells, we examined GFP-Smf1 levels in additional mutants containing blocks in the MVB pathway. Key elements of the MVB pathway are the ESCRT complexes that sort proteins destined for the vacuole into endosomes and the MVB

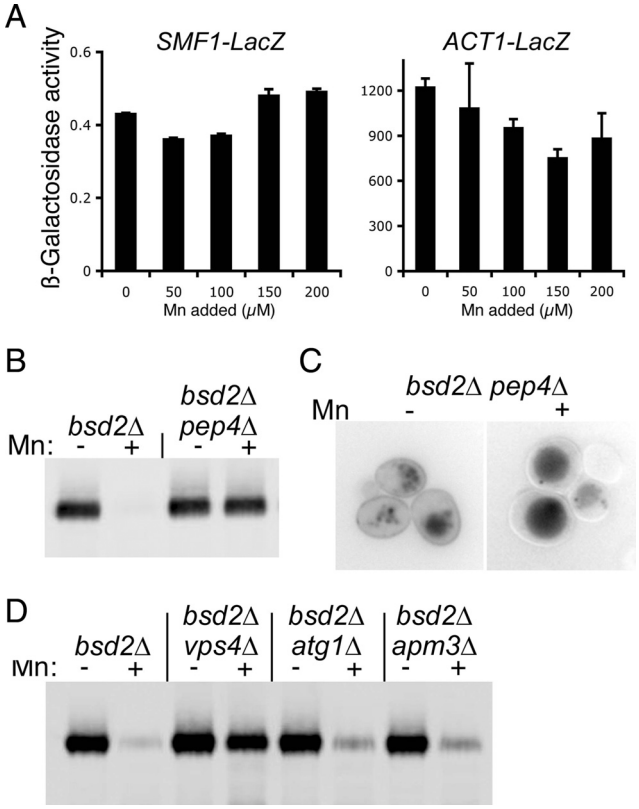

Figure 2. Regulation of Smf1p at toxic manganese is posttranslational and occurs through vacuolar degradation. (A) The promoters of *SMF1* and *ACT1* were fused to *LacZ* and expressed in WT cells treated for 16 h with the indicated concentration of manganese in YPD medium. ß-Galactosidase activity was measured using *o*-nitrophenyl ß-D-galactopyranoside (ONPG) as a substrate. Results are the averages of two trials; error, SD. (B–D) GFP-Smf1 was expressed in the indicated strains grown in YPD medium (−) or the same medium supplemented with 200 μM $MnCl_2$ (+) for 16 h. (B and D) The abundance of GFP-Smf1 was monitored using immunoblots. (C) Cellular localization of GFP-Smf1 was observed by fluorescence microscopy at 100× magnification. Strains utilized include WT, BY4741; *bsd2*Δ, 5738; *bsd2*Δ *pep4*Δ, LJ388; *bsd2*Δ *vps4*Δ, LJ389; *bsd2*Δ *atg1*Δ, LJ405; and *bsd2*Δ *apm3*Δ, LJ404.

(Williams and Urbe, 2007). We observed that blocking each of the ESCRT complexes individually using *vps23*Δ (ESCRT-I), *vps36*Δ (ESCRT-II), and *snf7*Δ (ESCRT-III) mutations in combination with *bsd2*Δ resulted in enhanced stability of GFP-Smf1 grown with exposure to toxic manganese (Figure 3A). In addition to the ESCRT complexes we monitored GFP-Smf1 levels in *bsd2*Δ yeast lacking genes involved in entry of proteins into (*PEP12* and *VPS21*; Gerrard *et al.*, 2000a,b) or exit from (*VPS27*) the prevacuolar compartment (Piper *et al.*, 1995), and again we observed a block in the manganese-induced degradation of Smf1p (Figure 3B). Localization of GFP-Smf1 in the *bsd2*Δ *vps27*Δ strain with toxic manganese is also consistent with a large endosome structure, most likely the class E compartment (Supplemental Figure S2). These results demonstrate that the MVB pathway is involved in targeting of Smf1p to the vacuole in cells grown in the presence of toxic manganese.

Smf1p has been localized to both the plasma membrane and in internal vesicles (Liu and Culotta, 1999b; Sullivan *et al.*, 2007). To determine if vacuolar targeting during manganese exposure involves one or both of these Smf1p locations, we utilized mutants that either blocked the endocytic pathway (*end3*Δ; Benedetti *et al.*, 1994) or Golgi-to-vacuolar trafficking (*vps45*Δ; Bryant *et al.*, 1998). We observed that blocking either endocytosis or Golgi to vacuolar transport was capable of inhibiting some degradation of Smf1p during exposure to toxic manganese (Figure 3C), yet effects of blocking Golgi to vacuolar transport were greater than that of blocking endocytosis (see legend Figure 3C). These results suggest that the Bsd2-independent vacuolar targeting of Smf1p largely involves protein derived from the exocytic pathway, but also from the endocytic pathway.

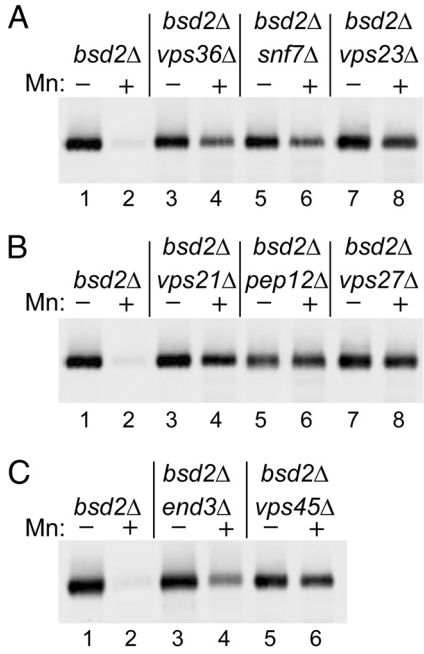

Figure 3. Degradation of Smf1p by toxic manganese is mediated by the MVB sorting pathway. (A–C) Levels of GFP-Smf1 were monitored by immunoblot in the designated strains grown in YPD medium supplemented where indicated (+) with 200 μM $MnCl_2$ for 16 h. Through quantitation of immunoblots in C using Odyssey software, the levels of GFP-Smf1 in manganese-treated cells was 5% (*bsd2*Δ), 39% (*bsd2*Δ *end3*Δ), and 69% (*bsd2*Δ *vps45*Δ) that of the corresponding cells not treated with manganese. Strains utilized include WT, BY4741; *bsd2*Δ, 5738; *bsd2*Δ *vps36*Δ, LJ387; *bsd2*Δ *snf7*Δ, LJ386; *bsd2*Δ *vps23*Δ, LJ390; *bsd2*Δ *vps21*Δ, LJ385; *bsd2*Δ *pep12*Δ, LJ395; *bsd2*Δ *vps27*Δ, LJ391; *bsd2*Δ *end3*Δ, LJ392; and *bsd2*Δ *vps45*Δ, LJ393.

Two Steps for Down-Regulating Smf1 by Toxic Manganese

The aforementioned studies with secretory pathway mutants suggests that both cell surface and intracellular Smf1p are subject to down-regulation by toxic manganese. In wild-type (WT) cells, steady-state Smf1p is predominantly intracellular, whereas in *bsd2*Δ mutants and also *tre1 tre2* mutants, the protein can accumulate at the cell surface (Liu and Culotta, 1999b; Stimpson *et al.*, 2006; Sullivan *et al.*, 2007; also see Figure 4B). We therefore analyzed Smf1p levels and localization in WT versus *bsd2*Δ cells as a function of time of manganese treatment. The experiments of Figures 1–3 were all conducted with long-term "chronic" manganese exposures (16 h). Yet we observed that the addition of toxic manganese to WT cells has no effect during short periods and requires 4 h to see any change in GFP-Smf1; even so Smf1p loss is no greater than 50% (Figure 4A, lane 7). By comparison, the response of GFP-Smf1 in *bsd2*Δ cells to toxic manganese is more rapid and GFP-Smf1 levels are reduced

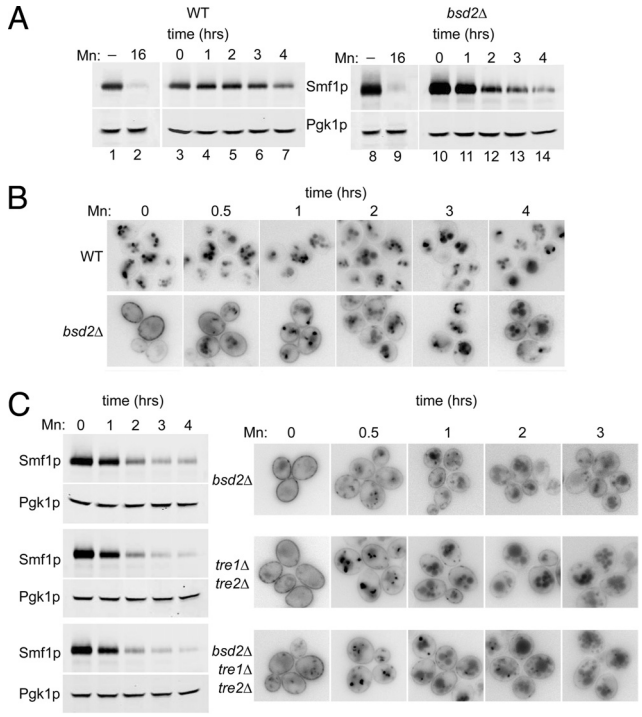

Figure 4. Two modes for down-regulating Smf1p by toxic manganese. (A) GFP-Smf1 levels were monitored from cells grown in YPD with no added metal (−, lanes 1 and 8) or the same medium supplemented with 200 μM $MnCl_2$ (16 h, lanes 2 and 9). Cultures were also grown in YPD to an OD 600 nm of ~1 and then supplemented with 200 μM $MnCl_2$ (lanes 3–7 and 10–14), and samples were removed at the indicated times after addition of manganese for immunoblot analysis. (B) Cellular localization of GFP-Smf1 was monitored using fluorescence microscopy at ×100 magnification. (C) GFP-Smf1 protein levels and cellular localization in *bsd2*Δ, *tre1*Δ *tre2*Δ, and *bsd2*Δ *tre1*Δ *tre2*Δ strains were monitored in cells grown in YPD as described in A and B. Strains utilized include WT, BY4741; *bsd2*Δ, 5738, *bsd2*Δ, LJ423; *tre1*Δ *tre2*Δ, *tre1/2*; and *bsd2*Δ *tre1*Δ *tre2*Δ, LJ420.

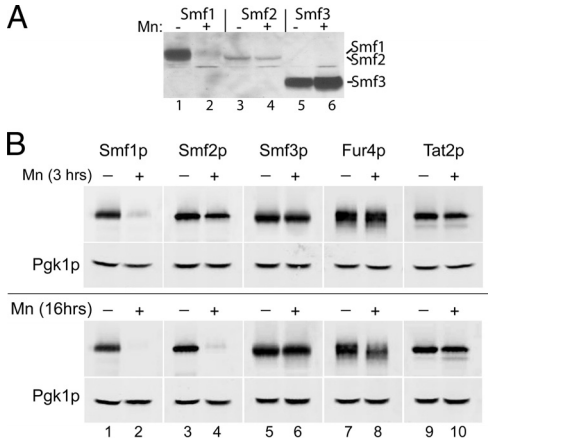

Figure 5. Toxic manganese preferentially down-regulates Smf1p (A) Immunoblot analysis comparison of the three Nramp transporters of yeast Smf1p, Smf2p, and Smf3p tagged at the C-terminus with HA and expressed from their native promoters in WT cells. Cultures were grown for 16 h in YPD with no added metal (−) or 200 μM $MnCl_2$ (+). (B) Smf1p, Smf2p, and Smf3p were tagged at the N-terminus with GFP and expressed from the *TPI1* promoter; Fur4p and Tat2p were tagged at the C-terminus with GFP and expressed from the *PGK1* promoter. Cultures of *bsd2*Δ cells were grown in YPD to an OD 600 nm of ~1 then supplemented with 200 μM $MnCl_2$ (top panel), samples were removed 3 h after addition of manganese for immunoblot analysis. Cells were also grown in YPD with no added metal (−) or the same medium supplemented with 200 μM $MnCl_2$ for 16 h as in A (bottom panel). Strains utilized include WT, BY4741; and *bsd2*Δ, 5738.

to ~20% within 2 h (Figure 4A, right). The differences seen in the rate of loss of GFP-Smf1 between WT and *bsd2*Δ yeast may be due to GFP-Smf1 localization. In WT cells, addition of toxic manganese does not significantly alter the punctate localization until 4 h of exposure when GFP-Smf1 begins to localize to the large round vacuoles (Figure 4B, top panel). In contrast, the effects of manganese on cell surface GFP-Smf1 in *bsd2*Δ cells is more rapid. Within 30 min of manganese treatment, plasma membrane GFP-Smf1 begins to be endocytosed and is fully internalized by 3 h (Figure 4B, bottom panel), and the same is true for GFP-Smf1 expressed in the *tre1*Δ *tre2*Δ and *bsd2*Δ *tre1*Δ *tre2*Δ triple mutants (Figure 4C). However, the internalized Smf1p does not appear to immediate concentrate within the large round vacuole; this requires prolonged exposures to the metal (>4 h as in Figure 2C). Hence, toxic manganese appears to affect Smf1p localization in two ways. First, there is a relatively rapid internalization of cell surface Smf1p as seen in *bsd2*Δ mutants, and second, intracellular Smf1p as accumulates in WT cells, moves toward to the vacuole during prolonged exposures to the metal.

We tested whether these dual effects of manganese can be expanded to other transporters. *Saccharomyces cerevisiae* Smf2p transports manganese, whereas Smf3p is the vacuolar transporter of iron (Portnoy *et al.*, 2000; Luk and Culotta, 2001). As seen in Figure 5A (lanes 3 and 4), Smf2-HA expressed from its native promoter is not normally down-regulated during chronic exposures to toxic manganese. However, Smf2p is expressed at very low levels compared with Smf1p (cf. lanes 1 and 3, Figure 5A) and when placed under control of the strong *TPI1* promoter, Smf2p did exhibit some toxic manganese regulation, but effects were only seen during chronic (Figure 5B, lanes 3 and 4, bottom panel), and not short-term (top panel) exposures to manganese. Smf2p may have some capacity to respond to toxic manganese, but only when expressed at nonphysiological high levels. Compared with Smf1p and Smf2p, Smf3p is not regulated by manganese under any conditions tested, either driven by its own promoter (Figure 5A, lane 6) or the *TPI1* promoter (Figure 5B, lane 6). We also tested the effects of manganese on the uracile permease Fur4p and the tryptophan/tyrosine permease Tat2p. The abundance of both Fur4-GFP and Tat2-GFP are not significantly changed by growth in the presence of toxic manganese (Figure 5B). Toxic manganese preferentially down-regulates Smf1p.

Previous studies have shown that regulation of Smf1p by physiological manganese (Stimpson *et al.*, 2006) or by cadmium (Nikko *et al.*, 2008) involves ubiquitination by the E3 ligase Rsp5p; we tested whether the same was true for toxic manganese regulation. To monitor the effects of *rsp5* we first used a temperature-sensitive *rsp5-1* allele. As seen in Figure 6A, the manganese-induced endocytosis of GFP-Smf1 in the *bsd2*Δ strain was attenuated by the *rsp5-1* mutation at the restrictive temperature. To test the effects of *RSP5* loss at longer chronic periods of manganese toxicity, we used a viable promoter mutant of *rsp5.* In this allele, the *HIS3* gene was inserted in the *RSP5* promoter to causes a dramatic reduction in Rsp5p levels; this mutant is similar to other *RSP5* promoter mutants containing insertion of a Ty element

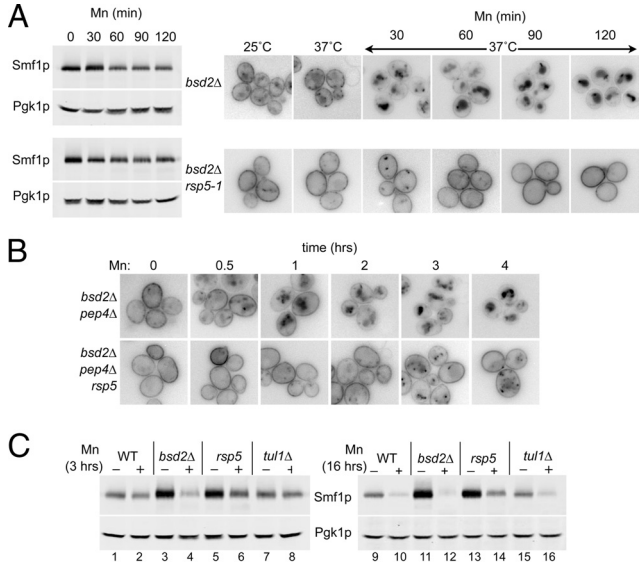

Figure 6. The role of the ubiquitin ligases *RSP5* and *TUL1* in the down-regulation of Smf1p during toxic manganese stress. (A) Cultures of *bsd2*Δ and *bsd2*Δ *rsp5-1* strains containing GFP-Smf1 were grown in YPD at 25°C to an $OD_{600\ nm}$ of ~1 then shifted to 37°C for 30 min before addition of 200 μM $MnCl_2$, and samples were removed at the indicated times. Immunoblot analysis and cellular localization of GFP-Smf1 was done as in Figure 4. (B) Cellular localization of GFP-Smf1 was monitored using fluorescence microscopy as in A but in *bsd2*Δ *pep4* or in a triple mutant containing an insertion of the *HIS3* gene within the promoter of *RSP5* (*bsd2*Δ *pep4*Δ *rsp5*). (C) Immunoblot analysis of GFP-Smf1 expressed in WT, *bsd2*Δ, *rsp5*, and *tul1*Δ grown in YPD alone (−) or supplemented with 200 μM $MnCl_2$ (+) for either 3 or 16 h as in Figure 5. Strains utilized include WT, BY4741; *bsd2*Δ, 5738; *rsp5*, LJ424; *tul1*Δ, 4883; *bsd2*Δ *pep4*Δ, LJ388; and *bsd2*Δ *pep4*Δ *rsp5*, LJ426; *bsd2*Δ, LJ431; *bsd2*Δ *rsp5-1*, LJ432.

(Hein *et al.*, 1995) or the *natMX* cassette (Nikko *et al.*, 2008). This mutant is indeed defective for Rsp5p because basal levels of GFP-Smf1 were increased in this *rsp5* mutant (Figure 6C, lanes 5 and 13) to the same degree as seen in a *bsd2*Δ null (lanes 3 and 11), demonstrating a block in Smf1p regulation by physiological manganese. Moreover, this *rsp5* promoter mutant mirrored the *ts rsp5-1* allele in that it inhibited manganese-induced endocytosis of Smf1p in *bsd2*Δ strains (Figure 6B). This viable *rsp5* mutant provided the added advantage of monitoring effects at prolonged manganese exposures. As seen in Figure 6C, lane 14, the GFP-Smf1 polypeptide was still down-regulated ≈70% during chronic exposure of the *rsp5* mutant to toxic manganese. Hence, Rsp5 appears necessary for manganese-induced endocytosis of Smf1p, but may not be as critical for vacuolar degradation of intracellular Smf1p during longer exposures to the metal. To this end, we tested whether the Tul1p E3 ligase may be required. As seen in Figure 6C, *tul1*Δ mutations had no effect on the down-regulation of Smf1p during chronic exposures to manganese (lane 16), implying an alternative mechanism.

The Smf1p N-Terminus and Toxic Manganese Regulation

We sought to determine sequences of Smf1p that modulate regulation during manganese toxicity. Smf1p and Smf2p contain N-terminal extensions that are absent in Smf3p, and in the case of Smf1p, residues K33 and K34 within this N-terminus were found to be involved in Smf1p regulation by cadmium (Nikko *et al.*, 2008). Specifically these residues were implicated in Rsp5p-mediated ubiquitination of Smf1p as a prelude to endocytosis (Nikko *et al.*, 2008). We tested whether these same residues were involved in toxic manganese regulation of Smf1p. As seen in Figure 7A, lane 7, the K33,34R variant of GFP-Smf1 was degraded to a degree similar to that of WT GFP-Smf1 under chronic (16 h) exposures to manganese. Moreover, under shorter periods of manganese toxicity, the protein was endocytosed (Figure 7B) and degraded (Figure 7A, lanes 2–5) with roughly the same kinetics as WT GFP-Smf1. Although these N-terminal lysines are not absolutely essential for manganese regulation, we did observe a requirement for the Smf1p N-terminus. As seen in Figure 7A, a Δ63 variant of GFP-Smf1 lacking the cytosolic N-terminus was not down-regulated during 4 h of manganese treatment (lanes 2–5), nor was the protein subject to any endocytosis during this period (Figure 7B). Nevertheless, Δ63 GFP-Smf1 did eventually exhibit some down-regulation by toxic manganese during chronic exposures (Figure 7A, lane 7, middle panel). The N-terminus appears to facilitate the rapid response to toxic manganese, and residues other than K33 and K34 are involved.

Sensing of Manganese for Regulating Smf1p by Manganese Starvation versus Manganese Toxicity

An attractive model for the manganese regulation of Smf1p involves Smf1p as a sensor itself whereby metal binding to the transporter signals targeting to the vacuole for degradation. To begin to address this, we tested whether metal transport activity was necessary for the regulation of Smf1p during chronic manganese toxicity.

Previous mutagenesis studies with bacterial and human Nramp transporters have identified conserved residues important for metal ion transport. On the basis of these findings, we introduced mutations D92G and E344A into TM1

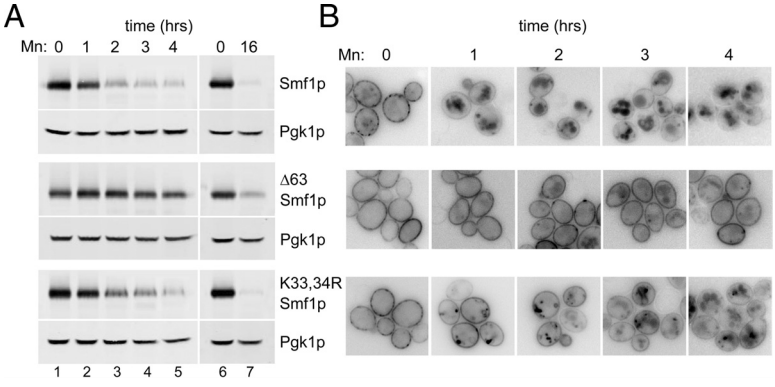

Figure 7. The N-terminus of Smf1p and the response to toxic manganese. The protein levels (A) and cellular localization (B) of wild type, Δ63, and K33,34R GFP-Smf1 were monitored in *bsd2*Δ cells grown in YPD as described in Figure 4. Strain *bsd2*Δ, 5738 was used in these experiments.

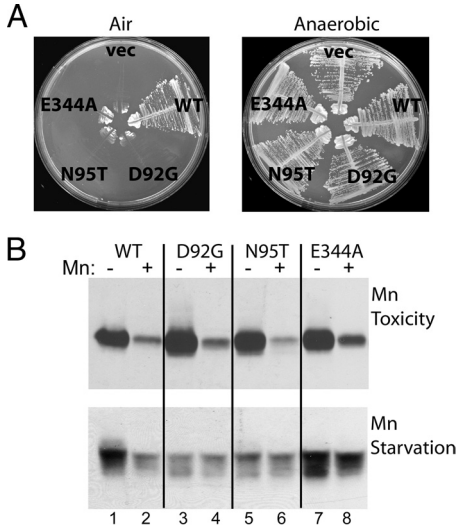

Figure 8. Effects of metal transport mutations on manganese regulation of Smf1p. (A) The ability of the indicated Smf1-HA mutants or WT Smf1-HA to complement a *smf1-1* mutation was tested. A *sod1*Δ *bsd2*Δ *smf1-1 is* unable to grow aerobically without lysine because of loss of Smf1p-transport of manganese-based antioxidants, which substitute for Cu/Zn SOD1 (Reddi *et al.,* 2009). Transformation with WT Smf1 complements this defect and allows for aerobic growth on medium lacking lysine (left), whereas the corresponding Smf1p mutants do not. (B) Smf1-HA and the D92G, N95T, and E344A derivatives were expressed in the WT BY4741 strain and protein abundance was monitored using immunoblots. Cultures were grown in YPD medium alone (−) or supplemented with 200 μM $MnCl_2$ (+; top panel) or in minimal defined medium depleted of manganese (−) or supplemented with 20 μM $MnCl_2$ (+) Bottom, strain ultilized include WT, BY4741; and *sod1*Δ *bsd2*Δ *smf1-1*, XBSBS1.

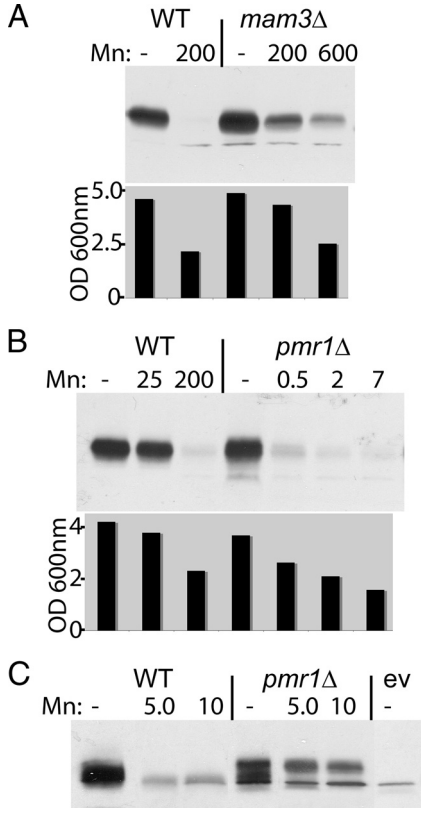

Figure 9. Smf1p is sensing intracellular manganese. (A–C) Smf1-HA was expressed in WT, *mam3*Δ, or *pmr1*Δ strains and protein abundance, and cell growth was monitored as in Figure 1. Cultures for A and B were grown in YPD medium, and the cells for C were grown in manganese-depleted minimal defined medium for 16 h. In each case the medium was supplemented with the indicated concentration of manganese (μM). ev, empty vector–transformed cells to illustrate position of nonspecific band cross-reacting with anti-HA. Strains utilized include WT, BY4741; *mam3*Δ, 1752; and *pmr1*Δ, 4534.

and TM8 of Smf1-HA, whose equivalent substitutions in human Nramp2 disrupt metal transport without affecting protein localization (Lam-Yuk-Tseung *et al.,* 2003). We also introduced N95T into Smf1p TM1, which was shown to disrupt manganese transport in *Escherichia coli* Nramp (Chaloupka *et al.,* 2005). All three Smf1-HA mutants were stably expressed in yeast (Figure 8B), yet were unable to complement the oxidative stress defect of a yeast *smf1* mutant (Figure 8A), a phenotype specifically associated with loss of Smf1p-manganese transport (Reddi *et al.,* 2009). Hence, these mutants are defective in Smf1-manganese transport in yeast. Nevertheless the three transport mutants were still down-regulated by chronic exposure to toxic manganese (Figure 8B, top panel), demonstrating that manganese transport is not necessary for this response to metal toxicity. We also tested whether the transport mutants affect the ability of Smf1p to respond to manganese starvation. WT Smf1-HA levels are normally increased during manganese starvation (Liu and Culotta, 1999b) as seen in Figure 8B (bottom panel, lane 2). However, all three manganese transport mutants were impaired in their ability to respond to changes in manganese starvation conditions (Figure 8B bottom panel). Smf1p mutants D92G and N95T fail to be upregulated with manganese starvation as was seen with other mutants that disrupt manganese transport (Liu and Culotta, 1999b). Levels of the E344A mutant also do not change with manganese starvation, although this Smf1p variant accumulates to overall higher levels. Smf1p transport activity seems important for regulation by very low, but not very high manganese.

What are the pools of manganese that are being sensed for Smf1p regulation? Because Smf1p localizes at both the cell surface and secretory pathway, Smf1p regulation could involve manganese pools that are extracellular, cytosolic, or intraluminal secretory pathway. To begin to resolve this, we tested Smf1p regulation in yeast mutants affecting manganese homeostasis. We have previously shown that yeast *mam3*Δ mutants accumulate lower cytosolic manganese under manganese surplus conditions and are resistant to manganese toxicity (Yang *et al.,* 2005). As seen in Figure 9A, it takes greater concentrations of manganese to down-regulate Smf1-HA in a *mam3*Δ mutant compared with the WT strain. Because it is intracellular and not extracellular manganese that is affected in *mam3*Δ mutants (Yang *et al.,* 2005), Smf1-HA is responding to an intracellular pool of toxic manganese during chronic manganese toxicity. Another mutant affecting cellular pools of manganese is *pmr1*. *PMR1* encodes a Golgi transporting ATPase for Mn. Mutants lacking Pmr1p accumulate high manganese in the cytosol and low Golgi manganese, and are exquisitely sensitive to manganese toxicity (Rudolph *et al.,* 1989; Lapinskas *et al.,* 1995; Durr *et al.,* 1998; Mandal *et al.,* 2000). As seen in Figure 9B, *pmr1*Δ mutants down-regulate Smf1-HA at much lower manganese concentrations than the WT strain. As such,

Smf1p appears to sense cytosolic or extra Golgi manganese during chronic manganese toxicity.

We also used the *pmr1*Δ mutant to test whether cytosolic or Golgi luminal manganese is being sensed with manganese starvation. In WT cells, Smf1-HA is normally expressed at high levels with manganese starvation, and down-regulated in response to 5–10 μM (nontoxic/physiological) levels of manganese (Figure 9C). Yet in a *pmr1*Δ mutant, there is no such response to manganese; the polypeptide remains at high levels (Figure 9C). Because a *pmr1*Δ mutant blocks manganese uptake into the secretory pathway, these studies indicate that under manganese starvation conditions, Smf1p is sensing intraGolgi manganese. Hence, the manganese for regulating Smf1p at manganese starvation and chronic manganese toxicity appears to arise from different cellular compartments.

DISCUSSION

Yeast cells respond to differential manganese exposures by altering the polypeptide levels and localization of the major Nramp manganese transporter Smf1p. Under manganese starvation, the transporter stably accumulates at the cell surface, whereas with physiological manganese, a bulk but not all of the protein is degraded in the vacuole via the MVB pathway. We now show that under manganese toxicity conditions, the remainder of Smf1p is also targeted to the MVB for vacuolar degradation, but through a distinct mechanism.

As we show for Smf1p, the Ftr1p iron transporter of yeast also undergoes two tiers of vacuolar degradation (Strochlic *et al.,* 2008). With physiological iron, Ftr1p is subject to "basal MVB sorting" and with higher iron levels, a "stimulated MVB sorting" occurs where a larger proportion of the transporter is degraded (Strochlic *et al.,* 2008). Both basal and stimulated MVB sorting of Ftr1p employ the same pathway involving ubiquitination by the E3 ligase Rsp5p (Strochlic *et al.,* 2008). Although Smf1p is similarly subject to basal and stimulated MVB sorting, distinct pathways are utilized. Basal MVB sorting with physiological manganese clearly involves recognition by Bsd2p/Tre1p/Tre2p, whereas stimulated MVB sorting at high manganese does not. Furthermore, basal MVB sorting of Smf1p clearly requires ubiquitination by Rsp5p, whereas a role for Rsp5p in stimulated MVB sorting of Smf1p is less obvious. Our studies thus far suggest that Rsp5p is required for manganese-induced endocytosis of Smf1p, but may not be required for ultimate delivery of Smf1p to the vacuole. However, since the *rsp5* mutants used in these studies are not nulls, we cannot totally exclude the possibility that a low level of Rsp5p is sufficient to trigger vacuolar targeting of Smf1p during manganese toxicity. In any case, the lack of a requirement for Bsd2p and Tre1/Tre2 demonstrate that basal and stimulated MVB targeting of Smf1p are distinct. The need for dual pathways may reflect the second Nramp transporter, Smf2p. Smf2p is subject to the same basal MVB, Bsd2p-mediated degradation as Smf1p (Portnoy *et al.,* 2000), but is not typically turned over with toxic manganese. Smf2p is critical for activating manganese enzymes in the cell (Luk and Culotta, 2001) and the use of a Bsd2-independent pathway for regulating Smf1p during toxic manganese may help keep Smf2p levels constant.

Proteins can enter the MVB through either endocytic (from cell surface) or exocytic (from Golgi) pathways. Our studies show that both pathways can contribute to Smf1p degradation during manganese toxicity, but the kinetics for the two are different. In the case of cell surface Smf1p that accumulates in *bsd2*Δ strains, treatment with toxic manganese can trigger complete endocytosis of the transporter within 1–3 h. But when steady-state Smf1p is largely intracellular, as with WT cells, the kinetics for vacuolar targeting are remarkably slow and require ≥4 h. Furthermore, the Smf1p that is endocytosed upon manganese treatment is not immediately targeted to the vacuole, but requires sustained metal exposures to reach the vacuolar lumen. It is possible that this endocytic Smf1p merges with exocytic Smf1p into the same "holding" pool of the transporter that is ultimately moved into the vacuole after prolonged periods of toxic manganese exposure. In any case, the kinetics are quite slow in comparison to other reports of vacuolar targeting of metal transporters. With yeast transporters for copper, zinc and iron, the response time for transporter endocyotsis and/or vacuolar targeting typically ranges from minutes to 2 h (Gitan and Eide, 2000b; Pena *et al.,* 2000; Felice *et al.,* 2005). Moreover, cadmium was recently shown to induce endocytosis of Smf1p within minutes and vacuolar degradation within 1–2 h (Nikko *et al.,* 2008). The degradation of Smf1p by toxic manganese, particularly in WT cells is indeed very slow. The rationale for this slow response may be based on the role of Smf1p in oxidative stress protection. Exceedingly high levels of manganese that approach toxicity can provide a unique benefit to cells by promoting formation of nonproteinacous manganese antioxidants (Archibald and Fridovich, 1981, 1982; Chang and Kosman, 1989; Al-Maghrebi *et al.,* 2002; Barnese *et al.,* 2008). In *S. cerevisiae*, Smf1p serves as the primary source of these manganese antioxidants (Reddi *et al.,* 2009), and therefore Smf1p can be both protective and detrimental in the face of high manganese. The immediate degradation of Smf1p during high manganese exposures may not always be advantageous.

Our studies with manganese accumulation mutants (i.e., *pmr1* and *mam3*) show that during chronic manganese toxicity, intracellular, presumably cytosolic pools of the metal are being sensed for down-regulation of Smf1p. As one possibility, the metal directly reacts with Smf1p in the secretory pathway to stimulate its movement to the vacuole. The manganese translocating residues of the transporter are not likely to be involved, as Smf1p mutants defective in manganese transport were still subject to toxic manganese regulation. Other, perhaps low-affinity manganese binding sites on Smf1p may trigger trafficking to the vacuole. Alternatively, manganese binding to an as-of-yet unidentified partner protein for Smf1p may direct vacuolar targeting in the face of manganese toxicity.

Lastly, these studies have provided evidence for distinct modes of manganese sensing under very high and very low manganese. Our experiments with *pmr1*Δ mutants disrupted for Golgi uptake of manganese indicate that under manganese starvation conditions, the cell senses intra-Golgi manganese for up-regulation of Smf1p. By comparison, manganese pools outside the secretory pathway, presumably cytosolic are being sensed for the strong down-regulation of Smf1p during long-term manganese toxicity. This separate compartmentalization for manganese sensing is logical when one considers the consequences of too much or too little manganese. During manganese starvation, the critical manganese sugar transferases of the Golgi are at risk for inactivation (Nakajima and Ballou, 1975; Parodi, 1979; Durr *et al.,* 1998). The cytosol on the other hand appears to be a prime target of manganese toxicity (Lapinskas, 1995; Durr *et al.,* 1998). The distinct compartmentalization for sensing extremes of metal starvation and metal toxicity are likely applicable to other transition metals that are both essential and potentially deleterious.

ACKNOWLEDGMENTS

We thank Hugh R.B. Pelham and Susan Michaelis (Johns Hopkins University) for their gifts of yeast strains and plasmids. In addition we thank Walter H. Watson and J. Michael McCaffery for their assistance with immunoblot analysis and fluorescence microscopy. This work was supported in part by the Johns Hopkins University (JHU) National Institute of Environmental Health Sciences (NIEHS) Center and by the National Institutes of Health Grant ES 08996 awarded to V.C.C. C.J.H. was supported by the JHU NIEHS training grant 07141, and M.D.H. was supported by a fellowship from the American Australian Association.

REFERENCES

Al-Maghrebi, M., Fridovich, I., and Benov, L. (2002). Manganese supplementation relieves the phenotypic deficits seen in superoxide-dismutase-null *Escherichia coli.* Arch. Biochem. Biophys. *402*, 104–109.

Archibald, F. S., and Fridovich, I. (1982). Investigations on the state of the manganese in *Lactobacillus plantarum.* Arch. Biochm. Biophys. *215*, 589–596.

Archibald, F. S., and Fridovich., I. (1981). Manganese and defenses against oxygen toxicity in *Lactobacillus plantarum.* J. Bacteriol. *145*, 422–451.

Barnese, K., Gralla, E. B., Cabelli, D. E., and Valentine, J. S. (2008). Manganous phosphate acts as a superoxide dismutase. J. Am. Chem. Soc. *130*, 4604–4606.

Benedetti, H., Raths, S., Crausaz, F., and Riezman, H. (1994). The END3 gene encodes a protein that is required for the internalization step of endocytosis and for actin cytoskeleton organization in yeast. Mol. Biol. Cell *5*, 1023–1037.

Bryant, N. J., Piper, R. C., Gerrard, S. R., and Stevens, T. H. (1998). Traffic into the prevacuolar/endosomal compartment of *Saccharomyces cerevisiae*: a VPS45-dependent intracellular route and a VPS45-independent, endocytic route. Eur. J. Cell Biol. *76*, 43–52.

Cellier, M., Prive, G., Belouchi, A., Kwan, T., Rodrigues, V., Chia, W., and Gros, P. (1995). Nramp defines a family of membrane proteins. Proc. Natl. Acad. Sci. USA *92*, 10089–10093.

Chaloupka, R., Courville, P., Veyrier, F., Knudsen, B., Tompkins, T. A., and Cellier, M. F. (2005). Identification of functional amino acids in the Nramp family by a combination of evolutionary analysis and biophysical studies of metal and proton cotransport in vivo. Biochemistry *44*, 726–733.

Chang, E. C., and Kosman, D. J. (1989). Intracellular Mn(II)-associated superoxide scavenging activity protects Cu, Zn superoxide dismutase-deficient *Saccharomyces cerevisiae* against dioxygen stress. J. Biol. Chem. *264*, 12172–12178.

Dancis, A. (1998). Genetic analysis of iron uptake in the yeast *Saccharomyces cerevisiae.* J. Pediatr. *132*, S24–S29.

Dancis, A., Klausner, R. D., Hinnebusch, A. G., and Barriocanal, J. G. (1990). Genetic evidence that ferric reductase is required for iron uptake in *S. cerevisiae.* Mol. Cell. Biol. *10*, 2294–2301.

Dunn, R., and Hicke, L. (2001). Domains of the Rsp5 ubiquitin-protein ligase required for receptor-mediated and fluid-phase endocytosis. Mol. Biol. Cell *12*, 421–435.

Durr, G., Strayle, J., Plemper, R., Elbs, S., Klee, S. K., Catty, P., Wolf, D. H., and Rudolph, H. K. (1998). The medial-Golgi ion pump Pmr1 supplies the yeast secretory pathway with Ca^{2+} and Mn^{2+} required for glycosylation, sorting, and endoplasmic reticulum-associated protein degradation. Mol. Biol. Cell *9*, 1149–1162.

Eguez, L., Chung, Y. S., Kuchibhatla, A., Paidhungat, M., and Garrett, S. (2004). Yeast Mn^{2+} transporter, Smf1p, is regulated by ubiquitin-dependent vacuolar protein sorting. Genetics *167*, 107–117.

Felice, M. R., De Domenico, I., Li, L., Ward, D. M., Bartok, B., Musci, G., and Kaplan, J. (2005). Post-transcriptional regulation of the yeast high affinity iron transport system. J. Biol. Chem. *280*, 22181–22190.

Gerrard, S. R., Bryant, N. J., and Stevens, T. H. (2000a). VPS21 controls entry of endocytosed and biosynthetic proteins into the yeast prevacuolar compartment. Mol. Biol. Cell *11*, 613–626.

Gerrard, S. R., Levi, B. P., and Stevens, T. H. (2000b). Pep12p is a multifunctional yeast syntaxin that controls entry of biosynthetic, endocytic and retrograde traffic into the prevacuolar compartment. Traffic *1*, 259–269.

Giacomini, A., Corich, V., Ollero, F. J., Squartini, A., and Nuti, M. P. (1992). Experimental conditions may affect reproducibility of the beta-galactosidase assay. FEMS Microbiol. Lett. *79*, 87–90.

Gietz, R. D., and Schiestl, R. H. (1991). Applications of high efficiency lithium acetate trasformation of intact yeast cells using single-stranded nucleic acids as carrier. Yeast *7*, 253–263.

Gitan, R. S., and Eide, D. J. (2000a). Zinc-regulated ubiquitin conjugation signals endocytosis of the yeast ZRT1 zinc transporter. Biochem. J. *346*, 329–336.

Gitan, R. S., and Eide, D. J. (2000b). Zinc-regulated ubiquitin conjugation signals endocytosis of the yeast ZRT1 zinc transporter. Biochem. J. *346*(Pt 2), 329–336.

Gitan, R. S., Shababi, M., Kramer, M., and Eide, D. J. (2003). A cytosolic domain of the yeast Zrt1 zinc transporter is required for its post-translational inactivation in response to zinc and cadmium. J. Biol. Chem. *278*, 39558–39564.

Guarente, L., and Mason, T. (1983). Heme regulates transcription of the *CYC1* gene of *S. cerevisiae* via an upstream activation site. Cell *32*, 1279–1286.

Gunshin, H., *et al.* (1997). Cloning and characterization of a mammalian proton-coupled metal-ion transporter. Nature *388*, 482–488.

Hein, C., Springael, J. Y., Volland, C., Haguenauer-Tsapis, R., and Andre, B. (1995). NPl1, an essential yeast gene involved in induced degradation of Gap1 and Fur4 permeases, encodes the Rsp5 ubiquitin-protein ligase. Mol. Microbiol. *18*, 77–87.

Hettema, E. H., Valdez-Taubas, J., and Pelham, H. R. (2004). Bsd2 binds the ubiquitin ligase Rsp5 and mediates the ubiquitination of transmembrane proteins. EMBO J. *23*, 1279–1288.

Hobbs, A. E., Srinivasan, M., McCaffery, J. M., and Jensen, R. E. (2001). Mmm1p, a mitochondrial outer membrane protein, is connected to mitochondrial DNA (mtDNA) nucleoids and required for mtDNA stability. J. Cell Biol. *152*, 401–410.

Huang, J., Reggiori, F., and Klionsky, D. J. (2007). The transmembrane domain of acid trehalase mediates ubiquitin-independent multivesicular body pathway sorting. Mol. Biol. Cell *18*, 2511–2524.

Iwai, Y. Y., Serpe, M., Haile, D., Yang, W., Kosman, D. J., Klausner, R. D., and Dancis, A. (1997). Homeostatic regulation of copper uptake in yeast via direct binding of MAC1 protein to upstream regulatory sequences of FRE1 and CTR1. J. Biol. Chem. *272*, 17711–17718.

Jungmann, J., Reins, H., Lee, J., Romeo, A., Hassett, R., Kosman, D., and Jentsch, S. (1993). MAC1, a nuclear regulatory protein related to Cu-dependent transcription factors is involved in Cu/Fe utilization and stress resistance in yeast. EMBO J. *13*, 5051–5056.

Lam-Yuk-Tseung, S., Govoni, G., Forbes, J., and Gros, P. (2003). Iron transport by Nramp2/DMT1, pH regulation of transport by 2 histidines in transmembrane domain 6. Blood *101*, 3699–3707.

Lapinskas, P. (1995). Characterization of genes involved in the homeostasis of oxygen free radicals and metal ions in *Saccharomyces cerevisiae.* Ph.D. Thesis, Baltimore, MD: Johns Hopkins University.

Lapinskas, P. J., Cunningham, K. W., Liu, X. F., Fink, G. R., and Culotta, V. C. (1995). Mutations in *PMR1* suppress oxidative damage in yeast cells lacking superoxide dismutase. Mol. Cell. Biol. *15*, 1382–1388.

Lapinskas, P. J., Lin, S. J., and Culotta, V. C. (1996). The role of the *Saccharomyces cerevisiae CCC1* gene in the homeostasis of manganese ions. Mol. Microbiol. *21*, 519–528.

Liu, J., Sitaram, A., and Burd, C. G. (2007). Regulation of copper-dependent endocytosis and vacuolar degradation of the yeast copper transporter, Ctr1p, by the Rsp5 ubiquitin ligase. Traffic *8*, 1375–1384.

Liu, X. F., and Culotta, V. C. (1999a). Mutational analysis of *Saccharomyces cerevisiae* Smf1p, a member of the Nramp family of metal transporters. J. Mol. Biol. *289*, 885–891.

Liu, X. F., and Culotta, V. C. (1999b). Post-translational control of Nramp metal transport in yeast: role of metal ions and the *BSD2* gene. J. Biol. Chem. *274*, 4863–4868.

Liu, X. F., Supek, F., Nelson, N., and Culotta, V. C. (1997). Negative control of heavy metal uptake by the *Saccharomyces cerevisiae BSD2* gene. J. Biol. Chem. *272*, 11763–11769.

Luk, E., and Culotta, V. C. (2001). Manganese superoxide dismutase in *S. cerevisiae* acquires its metal co-factor through a pathway involving the Nramp metal transproter, Smf2p. J. Biol. Chem. *276*, 47556–47562.

Luk, E., Yang, M., Jensen, L. T., Bourbonnais, Y., and Culotta, V. C. (2005). Manganese activation of superoxide dismutase 2 in the mitochondria of *Saccharomyces cerevisiae.* J. Biol. Chem. *280*, 22715–22720.

Mandal, D., Woolf, T. B., and Rao, R. (2000). Manganese selectivity of Pmr1, the yeast secretory pathway ion pump, is defined by residue Gln783 in transmembrane segment 6. J. Biol. Chem. *31*, 23933–23938.

Nakajima, T., and Ballou, C. E. (1975). Yeast manno-protein biosynthesis: solubilization and selective assay of four mannosyltransferases. Proc. Natl. Acad. Sci. USA *72*, 3912–3916.

Nikko, E., Sullivan, J. A., and Pelham, H. R. (2008). Arrestin-like proteins mediate ubiquitination and endocytosis of the yeast metal transporter Smf1. EMBO Rep. *9*, 1216–1221.

Parodi, A. J. (1979). Biosynthesis of yeast manno proteins. J. Biol. Chem. *254*, 8343–8352.

Pena, M. M., Puig, S., and Thiele, D. J. (2000). Characterization of the *Saccharomyces cerevisiae* high affinity copper transporter Ctr3. J. Biol. Chem. *275*, 33244–33251.

Petris, M. J., Smith, K., Lee, J., and Thiele, D. J. (2003). Copper-stimulated endocytosis and degradation of the human copper transporter, hCtr1. J. Biol. Chem. *278*, 9639–9646.

Piper, R. C., Cooper, A. S., Yang, H., and Stevens, T. H. (1995). VPS27 controls vacuolar and endocytic traffic through a prevacuolar compartment in *Saccharomyces cerevisiae*. J. Cell Biol. *131*, 603–617.

Portnoy, M. E., Jensen, L. T., and Culotta, V. C. (2002). The distinct methods by which manganese and iron regulate the Nramp transporters in yeast. Biochem. J. *362*, 119–124.

Portnoy, M.E., Liu, X.F., and Culotta, V.C. (2000). Saccharomyces cerevisiae expresses three functionally distinct homologues of the Nramp family of metal transporters. Mol. Cell. Biol. *20*, 7893–7902.

Raymond, C. K., Howald-Stevenson, I., Vater, C. A., and Stevens, T. H. (1992). Morphological classification of the yeast vacuolar protein sorting mutants: evidence for a prevacuolar compartment in class E vps mutants. Mol. Biol. Cell *3*, 1389–1402.

Reddi, A. R., Jensen, L. T., Naranuntarat, A., Rosenfeld, L., Leung, E., Shah, R., and Culotta, V. C. (2009). The overlapping roles of manganese and Cu/Zn SOD in oxidative stress protection. Free Radic. Biol. Med. *46*, 154–162.

Rudolph, H. K., Antebi, A., Fink, G. R., Buckley, C. M., Dorman, T. E., LeVitre, J., Davidow, L. S., Mao, J. I., and Moir, D. T. (1989). The yeast secretory pathway is perturbed by mutations in *PMR1*, a member of a Ca^{+2}-ATPase family. Cell *58*, 133–145.

Sikorski, R. S., and Hieter, P. (1989). A system of shuttle vectors and yeast host strains designed for efficient manipulation of DNA in *Saccharomyces ceresiviae*. Genetics *122*, 19–27.

Sherman, F., Fink, G.R., and Lawrence, C.W. (1978). Methods in yeast genetics, Cold Spring Harbor, NY: Cold Spring Harbor Laboratory Press.

Stimpson, H. E., Lewis, M. J., and Pelham, H. R. (2006). Transferrin receptor-like proteins control the degradation of a yeast metal transporter. EMBO J. *25*, 662–672.

Strochlic, T. I., Schmiedekamp, B. C., Lee, J., Katzmann, D. J., and Burd, C. G. (2008). Opposing activities of the Snx3-retromer complex and ESCRT proteins mediate regulated cargo sorting at a common endosome. Mol. Biol. Cell *19*, 4694–4706.

Sullivan, J. A., Lewis, M. J., Nikko, E., and Pelham, H. R. (2007). Multiple interactions drive adaptor-mediated recruitment of the ubiquitin ligase rsp5 to membrane proteins in vivo and in vitro. Mol. Biol. Cell *18*, 2429–2440.

Sundin, B. A., Chiu, C. H., Riffle, M., Davis, T. N., and Muller, E. G. (2004). Localization of proteins that are coordinately expressed with Cln2 during the cell cycle. Yeast *21*, 793–800.

Thomine, S., Wang, R., Ward, J. M., Crawford, N. M., and Schroeder, J. I. (2000). Cadmium and iron transport by members of a plant metal transporter family in *Arabidopsis* with homology to nramp genes. Proc. Natl. Acad. Sci. USA *97*, 4991–4996.

Williams, R. L., and Urbe, S. (2007). The emerging shape of the ESCRT machinery. Nat. Rev. Mol. Cell Biol. *8*, 355–368.

Yamaguchi-Iwai, Y., Stearman, R., Dancis, A., and Klausner, R. D. (1996). Iron-regulated DNA binding by the AFT1 protein controls the iron regulon in yeast. EMBO J. *15*, 3377–3384.

Yang, M., Jensen, L. T., Gardner, A. J., and Culotta, V. C. (2005). Manganese toxicity and *Saccharomyces cerevisiae* Mam3p, a member of the ACDP (ancient conserved domain protein) family. Biochem J. *386*, 479–487.

Zhao, H., and Eide, D. (1997). Zap1p, a metalloregulatory protein involved in zinc-responsive transcriptional regulation in *Saccharomyces cerevisiae*. Mol. Cell. Biol. *17*, 5044–5052.